Stem Cell Reports, Volume *14*

Supplemental Information

Single-Cell Analysis Reveals Partial Reactivation of X Chromosome instead of Chromosome-wide Dampening in Naive Human Pluripotent Stem Cells

Susmita Mandal, Deepshikha Chandel, Harman Kaur, Sudeshna Majumdar, Maniteja Arava, and Srimonta Gayen

Single Cell Analysis Reveals Partial Reactivation of X-chromosome Instead of Chromosome-wide Dampening in Naïve Human Pluripotent Stem Cells

Mandal S[1], Chandel D[1], Kaur H, Majumdar S, Arava M, and Gayen S*

A

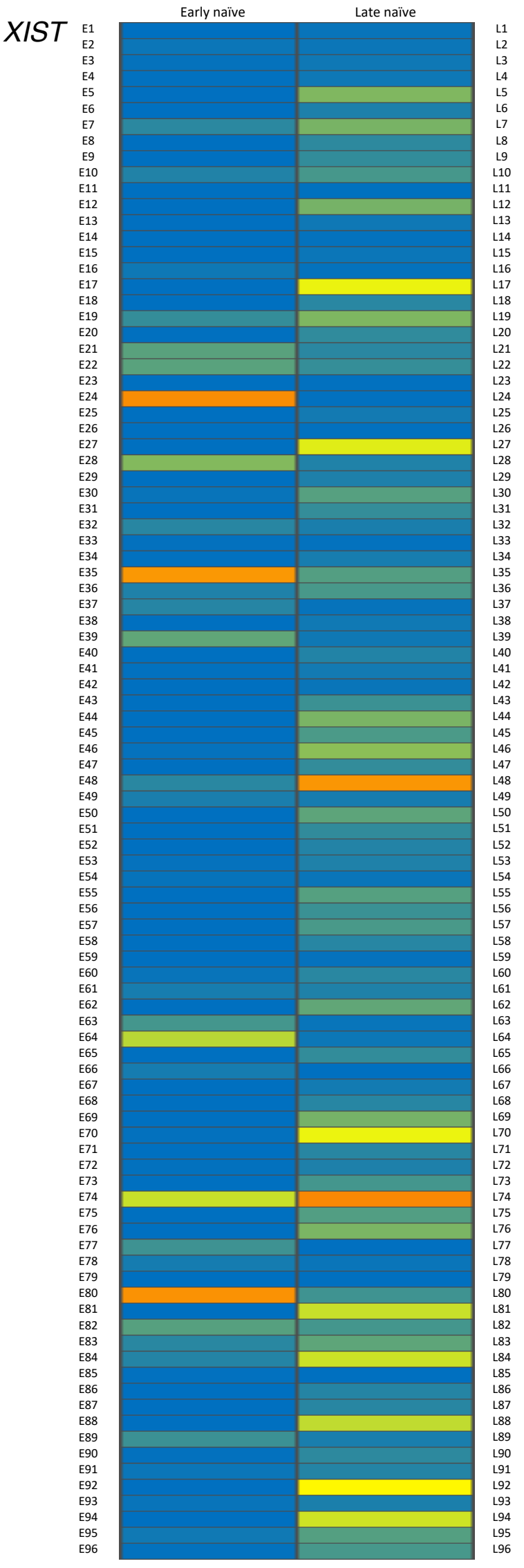
XIST
Early naïve
Late naïve
E1 E2 E3 E4 E5 E6 E7 E8 E9 E10 E11 E12 E13 E14 E15 E16 E17 E18 E19 E20 E21 E22 E23 E24 E25 E26 E27 E28 E29 E30 E31 E32 E33 E34 E35 E36 E37 E38 E39 E40 E41 E42 E43 E44 E45 E46 E47 E48 E49 E50 E51 E52 E53 E54 E55 E56 E57 E58 E59 E60 E61 E62 E63 E64 E65 E66 E67 E68 E69 E70 E71 E72 E73 E74 E75 E76 E77 E78 E79 E80 E81 E82 E83 E84 E85 E86 E87 E88 E89 E90 E91 E92 E93 E94 E95 E96
L1 L2 L3 L4 L5 L6 L7 L8 L9 L10 L11 L12 L13 L14 L15 L16 L17 L18 L19 L20 L21 L22 L23 L24 L25 L26 L27 L28 L29 L30 L31 L32 L33 L34 L35 L36 L37 L38 L39 L40 L41 L42 L43 L44 L45 L46 L47 L48 L49 L50 L51 L52 L53 L54 L55 L56 L57 L58 L59 L60 L61 L62 L63 L64 L65 L66 L67 L68 L69 L70 L71 L72 L73 L74 L75 L76 L77 L78 L79 L80 L81 L82 L83 L84 L85 L86 L87 L88 L89 L90 L91 L92 L93 L94 L95 L96

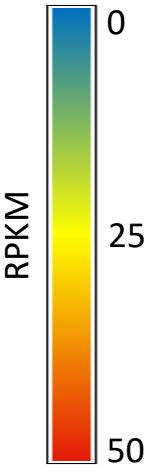
RPKM
0
25
50

B

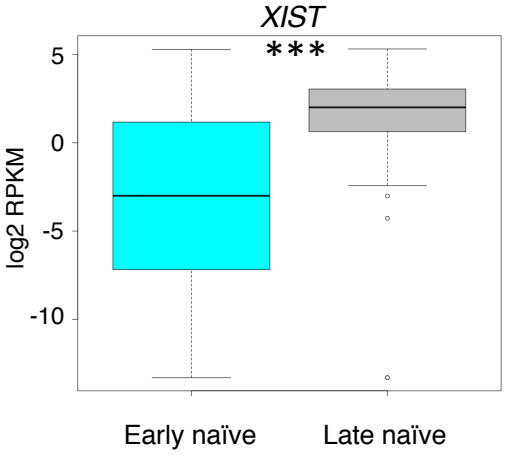
XIST
***
log2 RPKM
5
0
-5
-10
Early naïve
Late naïve

Figure S1, related to figure 1: Transition of early naïve to late naïve state is associated with increased *XIST* expression. (A) Heatmap representing the *XIST* expression (RPKM) in early naïve (n=96 cells) and late naïve cells (n=96 cells). (B) Comparison of *XIST* expression between early naïve (n=96 cells) and late naïve cells (n=96 cells). $p<0.00001$ (Mann-Whitney U-test).

A

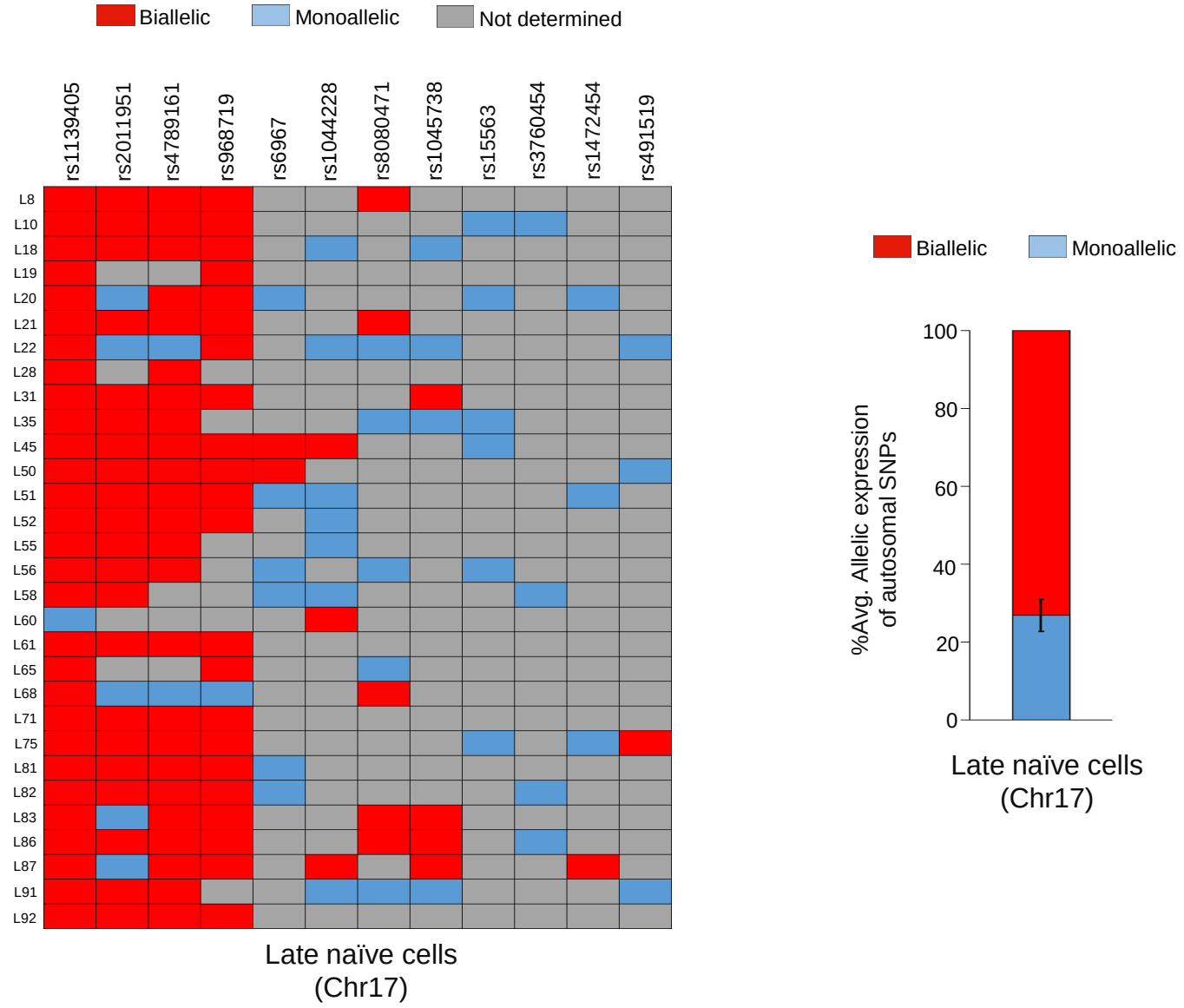
Biallelic
Monoallelic
Not determined
rs1139405
rs2011951
rs4789161
rs968719
rs6967
rs1044228
rs8080471
rs1045738
rs15563
rs3760454
rs1472454
rs491519
L8
L10
L18
L19
L20
L21
L22
L28
L31
L35
L45
L50
L51
L52
L55
L56
L58
L60
L61
L65
L68
L71
L75
L81
L82
L83
L86
L87
L91
L92
Late naïve cells
(Chr17)
Biallelic
Monoallelic
%Avg. Allelic expression
of autosomal SNPs
100
80
60
40
20
0
Late naïve cells
(Chr17)

B

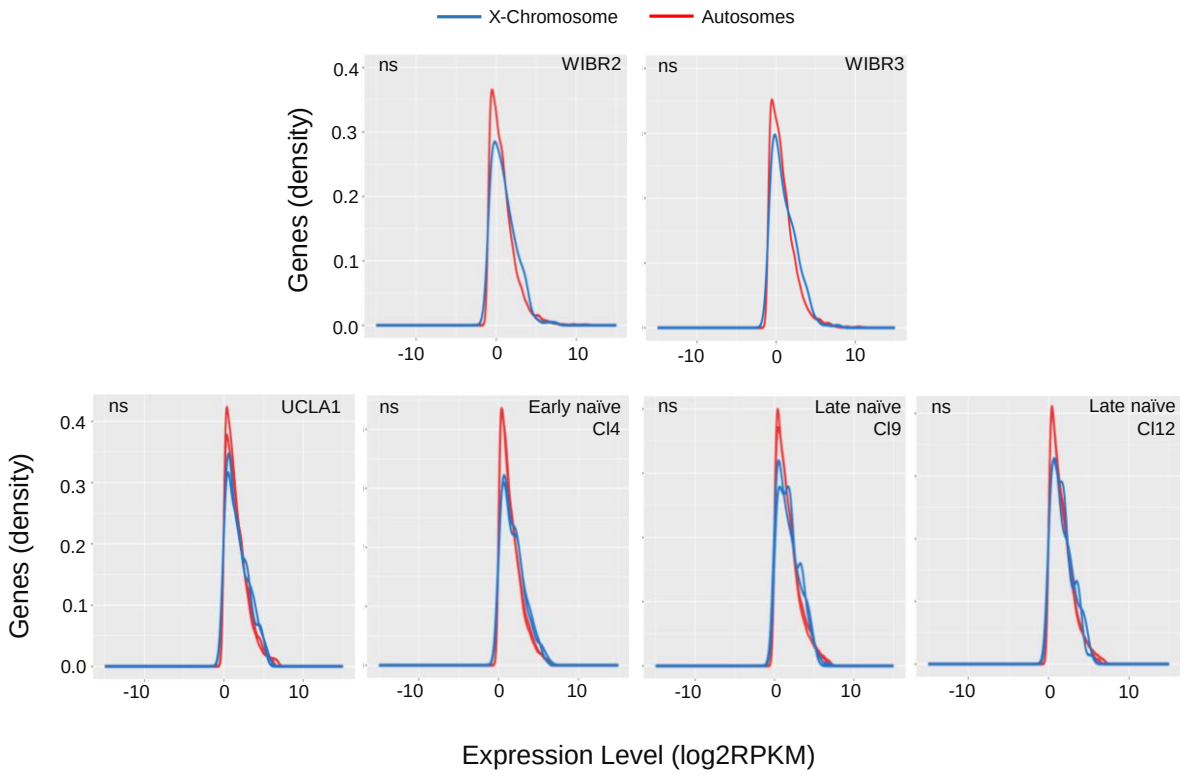
X-Chromosome
Autosomes
Genes (density)
ns
WIBR2
WIBR3
UCLA1
Early naïve
Cl4
Late naïve
Cl9
Late naïve
Cl12
0.4
0.3
0.2
0.1
0.0
-10
0
10
Expression Level (log2RPKM)

Figure S2, related to figure 3 and figure 4: (A) Allelic expression analysis of autosomal genes (Chr17) in late naïve cells (n=30 cells). Right, histogram showing the quantification of average percent of SNPs showing monoallelic and biallelic in late naïve cells. (B) Histograms showing that there were no significant difference between X-linked and autosomal gene expression distribution for WIBR2, WIBR3, UCLA1 primed, UCLA1 early naïve and UCLA1late naïve cells. ($p > 0.05$, by Kolmogorov-Smirnov test). Replicates of RNA-Seq dataset used: WIBR2 and WIBR3 (n=1); UCLA1, early naïve cl4, late naïve cl9, late naïve cl12 (n=2).

Supplementary file legends

Table S1: Analysis of X-linked gene expression in early and late naïve cells. Related to Figure 1

Table S2: Allelic analysis of *XIST* expression and comparison of X-linked gene expression in *XIST*-monoallelic, -biallelic and -negative cells of late naïve state. Related to Figure 2

Table S3: Allelic analysis of X-linked genes and autosomal genes (Chr17) in early and late naïve cells. Related to Figure 3

Table S4: Analysis of X-chromosomal ploidy in early and late naïve cells. Related to Figure 3

Table S5: RPKM of X-linked and autosomal genes used for X:A ratio analysis. Related to Figure 4

Supplemental experimental procedures

Data acquisition: For active X-chromosome upregulation analysis (related to Fig. 4), we used following datasets from bulk-population RNA-Seq: hESCs (H1) / 3iL hESCs (H1) -E-MTAB-2031(Chan et al., 2013), WIBR1, WIN1, WIBR2, WIBR3- GSE75868 (Theunissen et al., 2016), WIS2-GSE60138 (Irie et al., 2015), UCLA2- GSE88933 (Patel et al., 2017), H1_A-GSE85331 (Liu et al., 2017), HUES8 - GSE102311(Sun et al., 2018), HNES1_A, HNES1_B - E-MTAB-5674 (Guo et al., 2017), HNES1_C-E-MTAB-4461(Guo et al., 2016), 4iLIF H1, Lis1-GSE60955 (Sperber et al., 2015), H1_B-GSE75748 (Chu et al., 2016). For hESCs (Sc) - GSE36552 (Yan et al., 2013), we used single cell RNA-Seq dataset of 8 single cells.

Origin of naïve hPSCs: WIN1: Embryo derived, cultured in either 5i/L/A or 4i/L/A medium (Theunissen et al., 2016); 3iL hESCs: converted from hESCs (H1) using 3iL media (Chan et al., 2013); HNES1_A / B / C: Embryo derived, cultured in t2iLGO in different feeder conditions (Guo et al., 2016, 2017); 4iLIF H1: converted from H1 using 4iLIF media (Sperber et al., 2015); NHSM Lis1: Embryo derived, cultured in NHSM media (Sperber et al., 2015).

Reads mapping and counting: Reads were mapped to the human genome (hg38) using STAR (Dobin et al., 2013). Mapped reads were then processed using SAM tools (Li et al., 2009) and the number of reads mapping to each gene was counted using HTSeq-count (Anders et al., 2015).

Expression analysis of *XIST* and X-linked genes in early vs late naïve cells: We calculated RPKM (Reads Per Kilobase per Million) using rpkmforgenes (Ramsköld et al., 2009). First, we checked *XIST* expression in 192 single cells consisting of 96 early naïve and 96 late naive cells. Then, for early naive cells we selected 60 cells out of 96 showing very low *XIST* expression (0 to 0.5 RPKM) and then from these 60 cells we selected top 28 early cells having RPKM sum (2634.96 to 1267.39) and mean (> 0.9) for further analysis. For late naive cells, we selected 59 out of 96 showing very high *XIST* expression (3 to 39 RPKM) and then from these 59 cells we selected top 30 cells having RPKM sum (1949.62 to 1195.90) and mean (> 0.9) for further analysis. To check the expression of X-linked genes in (28 early naive + 30 late naive cells), we considered only those genes which were having $5 < \mu_{RPKM} < 200$.

Expression analysis of X-linked genes in *XIST*-biallelic, -monoallelic and -negative late naïve cells: For this analysis, 59 cells were selected out of 96 late naive cells based on the higher *XIST* expression (3 - 39 RPKM). Out of these 59 cells, 35 cells (RPKM sum >500; RPKM mean > 0.4) had allelic data for *XIST*. Allelic expression analysis for *XIST* was

performed as described in allelic expression analysis method section. Out of these 35 cells, 26 cells having monoallelic expression and 9 cells having biallelic expression for *XIST* were chosen for X-linked gene expression analysis. 17 *XIST* negative cells were selected based on *XIST* RPKM<1 and having RPKM sum >500; RPKM mean > 0.4. X-linked genes for expression analysis were chosen based on the $5 < \mu_{RPKM} < 200$.

Ploidy: To analyze the X-chromosomal ploidy, we considered 70 genes having RPKM mean ≥ 3 distributed across the X-chromosome for 58 cells (28 early naive cells + 30 late naive cells). We calculated gene expression ratio through dividing the individual gene's RPKM by its median value across all the 58 cells. To visualize the profile of X-chromosome in all these cells, the normalised gene expression values (gene expression ratio) were used to build a moving average plot (neighbourhood size, k=9) using methods described by Mayshar *et al.* (Mayshar et al., 2010).

X-chromosome to autosomes expression ratio: We calculated X:A ratio by dividing the median expression (RPKM) of the X-linked genes by the median expression (RPKM) of autosomal genes. For this analysis we removed the no/low expressed genes and considered the genes having ≥ 0.5 RPKM for both X and autosomal genes. We decided this threshold, based on the previous reports showing that exclusion of low expressed genes below 0.5 FPKM are more appropriate for assaying the active-X chromosome upregulation (Deng et al., 2011; Li et al., 2017; Sangrithi et al., 2017; Yildirim et al., 2012). We also profiled the expression level distribution of X-linked and autosomal genes as density plots created in R using the ggplot2 package. However, for analysis of X:A ratio of UCLA1 primed, early naïve and late naïve cells, we considered the expressed genes with RPKM ≥1 and upper RPKM threshold that corresponded to the lowest 99th centile RPKM value of expression to avoid the difference between X-linked and autosomal gene expression distribution. We excluded escapees and genes in the pseudo autosomal regions of X-chromosome for our analysis.

Statistical tests and Box-plots: All statistical tests and boxplots were performed using R version 3.5.1(R Development Core Team, 2016).

Supplemental References:

Anders, S., Pyl, P.T., and Huber, W. (2015). HTSeq-A Python framework to work with high-throughput sequencing data. Bioinformatics *31*, 166–169.

Chan, Y.S., Göke, J., Ng, J.H., Lu, X., Gonzales, K.A.U., Tan, C.P., Tng, W.Q., Hong, Z.Z., Lim, Y.S., and Ng, H.H. (2013). Induction of a human pluripotent state with distinct regulatory circuitry that resembles preimplantation epiblast. Cell Stem Cell *13*, 663–675.

Chu, L.F., Leng, N., Zhang, J., Hou, Z., Mamott, D., Vereide, D.T., Choi, J., Kendziorski, C., Stewart, R., and Thomson, J.A. (2016). Single-cell RNA-seq reveals novel regulators of human embryonic stem cell differentiation to definitive endoderm. Genome Biol. *17*.

Deng, X., Hiatt, J.B., Nguyen, D.K., Ercan, S., Sturgill, D., Hillier, L.W., Schlesinger, F., Davis, C.A., Reinke, V.J., Gingeras, T.R., et al. (2011). Evidence for compensatory upregulation of expressed X-linked genes in mammals, Caenorhabditis elegans and Drosophila melanogaster. Nat. Genet. *43*, 1179–1185.

Dobin, A., Davis, C.A., Schlesinger, F., Drenkow, J., Zaleski, C., Jha, S., Batut, P., Chaisson, M., and Gingeras, T.R. (2013). STAR: Ultrafast universal RNA-seq aligner. Bioinformatics *29*, 15–21.

Guo, G., Von Meyenn, F., Santos, F., Chen, Y., Reik, W., Bertone, P., Smith, A., and Nichols, J. (2016). Naive Pluripotent Stem Cells Derived Directly from Isolated Cells of the Human Inner Cell Mass. Stem Cell Reports *6*, 437–446.

Guo, G., von Meyenn, F., Rostovskaya, M., Clarke, J., Dietmann, S., Baker, D., Sahakyan, A., Myers, S., Bertone, P., Reik, W., et al. (2017). Epigenetic resetting of human pluripotency. Dev. *144*, 2748–2763.

Irie, N., Weinberger, L., Tang, W.W.C., Kobayashi, T., Viukov, S., Manor, Y.S., Dietmann, S., Hanna, J.H., and Surani, M.A. (2015). SOX17 is a critical specifier of human primordial germ cell fate. Cell *160*, 253–268.

Li, H., Handsaker, B., Wysoker, A., Fennell, T., Ruan, J., Homer, N., Marth, G., Abecasis, G., and Durbin, R. (2009). The Sequence Alignment/Map format and SAMtools. Bioinformatics *25*, 2078–2079.

Li, X., Hu, Z., Yu, X., Zhang, C., Ma, B., He, L., Wei, C., and Wu, J. (2017). Dosage compensation in the process of inactivation/reactivation during both germ cell development and early embryogenesis in mouse. Sci. Rep. *7*.

Liu, Q., Jiang, C., Xu, J., Zhao, M.T., Van Bortle, K., Cheng, X., Wang, G., Chang, H.Y., Wu, J.C., and Snyder, M.P. (2017). Genome-Wide Temporal Profiling of Transcriptome and

Open Chromatin of Early Cardiomyocyte Differentiation Derived from hiPSCs and hESCs. Circ. Res. *121*, 376–391.

Mayshar, Y., Ben-David, U., Lavon, N., Biancotti, J.C., Yakir, B., Clark, A.T., Plath, K., Lowry, W.E., and Benvenisty, N. (2010). Identification and classification of chromosomal aberrations in human induced pluripotent stem cells. Cell Stem Cell *7*, 521–531.

Patel, S., Bonora, G., Sahakyan, A., Kim, R., Chronis, C., Langerman, J., Fitz-Gibbon, S., Rubbi, L., Skelton, R.J.P., Ardehali, R., et al. (2017). Human Embryonic Stem Cells Do Not Change Their X Inactivation Status during Differentiation. Cell Rep. *18*, 54–67.

R Development Core Team (2016). R: A language and environment for statistical computing. R Found. Stat. Comput.

Ramsköld, D., Wang, E.T., Burge, C.B., and Sandberg, R. (2009). An abundance of ubiquitously expressed genes revealed by tissue transcriptome sequence data. PLoS Comput. Biol. *5*, e1000598.

Sangrithi, M.N., Royo, H., Mahadevaiah, S.K., Ojarikre, O., Bhaw, L., Sesay, A., Peters, A.H.F.M., Stadler, M., and Turner, J.M.A. (2017). Non-Canonical and Sexually Dimorphic X Dosage Compensation States in the Mouse and Human Germline. Dev. Cell *40*, 289–301.e3.

Sperber, H., Mathieu, J., Wang, Y., Ferreccio, A., Hesson, J., Xu, Z., Fischer, K.A., Devi, A., Detraux, D., Gu, H., et al. (2015). The metabolome regulates the epigenetic landscape during naive-to-primed human embryonic stem cell transition. Nat. Cell Biol. *17*, 1523–1535.

Sun, C., Zhang, J., Zheng, D., Wang, J., Yang, H., and Zhang, X. (2018). Transcriptome variations among human embryonic stem cell lines are associated with their differentiation propensity. PLoS One *13*.

Theunissen, T.W., Friedli, M., He, Y., Planet, E., O'Neil, R.C., Markoulaki, S., Pontis, J., Wang, H., Iouranova, A., Imbeault, M., et al. (2016). Molecular Criteria for Defining the Naive Human Pluripotent State. Cell Stem Cell *19*, 502–515.

Yan, L., Yang, M., Guo, H., Yang, L., Wu, J., Li, R., Liu, P., Lian, Y., Zheng, X., Yan, J., et al. (2013). Single-cell RNA-Seq profiling of human preimplantation embryos and embryonic stem cells. Nat. Struct. Mol. Biol. *20*, 1131–1139.

Yildirim, E., Sadreyev, R.I., Pinter, S.F., and Lee, J.T. (2012). X-chromosome

hyperactivation in mammals via nonlinear relationships between chromatin states and transcription. Nat. Struct. Mol. Biol. *19*, 56–62.